Furan−Formic Acid Dimers: An ab Initio and Matrix Isolation Study

Elsa Sánchez-García,[†] Arthur Mardyukov,[†] Marc Studentkowski,[†] Luis A. Montero,[‡] and Wolfram Sander*[,†]

Lehrstuhl für Organische Chemie II, Ruhr-Universität Bochum, D-44780 Bochum, Germany, and Laboratorio de Química Computacional y Teórica, Facultad de Química, Universidad de la Habana, 10400, Cuba

Received: August 7, 2006; In Final Form: October 19, 2006

The dimers formed by formic acid (FA) and furan are investigated by ab initio methods and matrix isolation spectroscopy. Nine complexes with binding energies between −3.91 and −0.82 kcal/mol (MP2/6-311++G-(d,p) + ZPE + BSSE) are identified. Another five weaker bound complexes are localized at lower level of theory only. The binding in the furan−FA dimers can be described in terms of OH···O, C═O···H, HO···H, CH···O, OH···π, and CH···π interactions. Therefore, the furan−FA complexes are classified in two types: (1) the dimers where the OH hydrogen of formic acid interacts with the furan molecule and (2) the dimers where the main interactions of FA with the furan molecule are via the less acidic CH hydrogen. Duning's and Pople's triple and double basis sets were used to study the dependence of the geometries and energies of the complexes from the basis set. BSSE (basis set superposition error) counterpoise corrections (CP) were included during the geometry optimizations of all dimers at the MP2/6-31G(d,p) level of theory. Matrix isolation spectroscopy allowed us to record the IR spectrum of aggregates between FA and furan. By comparison of the experimental IR spectrum with calculated IR spectra of a variety of complexes, it was possible to identify the most stable furan−FA dimer as the major product of the aggregation.

Introduction

Furan is an aromatic heterocyclic compound with many applications in different fields of chemistry from natural product synthesis to material science.[1] Therefore, furan, its aggregates, and complexes with small molecules have been subject to many experimental and theoretical studies.[2−18] The complexes of furan with hydrogen halides and alkynes have been investigated by Ault[13] and DeLaat and Ault[18] using matrix isolation spectroscopy. The equilibrium structures of the furan dimers and the nature of their intermolecular interactions were studied by Pei and Li using density functional theory and the natural bond orbital analysis.[2] The π···π interactions in the parallel, sandwich-shaped furan dimer have been analyzed using high-level ab initio theory.[19] The excited states of furan and the rotational spectra of some of its complexes with halides were also investigated.[6,7,9] Chan et al. studied the reactions of various acids with furan as part of their research about the preferred sites of protonation and hydrogen bonding for a set of basic substrates.[20]

Many studies of the interactions of furan with other molecules were focused on the furan−hydrogen halide complexes.[4,7,13] Legon and Millen[21,22] proposed a general rule to predict the geometry of B−HX complexes (X: F, Cl, Br, I, CN, CCH): if the Lewis base carries both *n* pairs and π electrons, the angular geometry is determined by the *n* pair rather than by the π electrons, and the Lewis acid lies along the axis of the *n* pair. Since the furan molecule contains both an *n* pair and π electrons, several studies of furan−HX complexes have been carried out to determine whether or not this rule is obeyed.[4,7,9] Cole et al.[7] studied the rotational spectrum of furan−HCl and HBr and showed that, while the HCl complex obeys Legon's rule, the HBr complex behaves differently and interacts with the π system of furan. Huang et al.[4] used ab-initio calculations to get insight into the binding situation of furan−HX complexes.

Formic acid (FA) as hydrogen bond donor and acceptor provides a good model to understand the variety of hydrogen bond interactions: from classical, strong interactions to weaker, nonclassical interactions.[23−30] The proton-transfer mechanism of the FA dimer has been extensively described,[26,31,32] and studies of the complexes of FA with other molecules like acetylene, water, dimethyl ether, and formamide were carried out in our group using matrix isolation spectroscopy in combination with ab-initio methods.[33−37]

In the present work, we describe the structures of the furan−FA complexes and discuss their binding energies and the influence of the basis set superposition errors (BSSE) on their geometries. The calculated vibrational spectra of the furan−FA dimers are compared to experimental matrix isolation IR spectra. The furan−FA system exhibits both *n* and π hydrogen bonding interactions. Therefore, the study of the furan−FA complexes leads to a detailed understanding of the noncovalent interaction in this type of systems.

Experimental Section

Matrix isolation experiments were performed by standard techniques using an APD CSW-202 Displex closed cycle helium refrigerator. Formic acid (Acros Organics) was distilled two times, was dried over molecular sieve (4 Å), and was degassed several times by the freeze−pump−thaw method before mixing with argon. Formic acid (FA) and furan were premixed with argon in a steel-mixing chamber using standard manometric methods. About 0.5−2 mbar of FA was mixed with 0.5−6 mbar of furan and was diluted with 1000−1500 mbar of argon in a 2-L glass bulb. Deposition was done on a CsI substrate at 10

* Author to whom correspondence should be addressed. Fax: +49 234 3214353. E-mail: wolfram.sander@rub.de.
[†] Ruhr-Universität Bochum.
[‡] Universidad de la Habana

10.1021/jp065064w CCC: $33.50
Published on Web 12/21/2006

K. The matrix was annealed at 30 and 35 K by staying at that temperature for up to 60 min and was cooled back to 10 K before recording spectra. Spectra were recorded on a Bruker IFS 66 FTIR spectrometer at 0.5 cm $^{-1}$ resolution in the range of 400−4000 cm^{-1}.

Computational Methods

The multiple minima hypersurface (MMH) approach[33,34,36−39] was used for searching configurational minima in the furan−FA system. One thousand randomly arranged furan−FA clusters were generated as starting point, and the resulting geometries were optimized and analyzed using PM3 and AM1[40−43] semiempirical quantum mechanical Hamiltonians.

These semiempirical results provided a preliminary overview of the furan−FA interactions, and the relevant configurations were further refined using ab-initio methods at various levels of theory.

The ab-initio computations were performed using the Gaussian 98[44] and Gaussian 03[45] programs. The equilibrium geometries and vibrational frequencies were calculated at the SCF level including second-order Møller-Plesset perturbation theory, MP2.[46] Pople's 6-31G(d,p) basis set,[47,48] the extended valence triple ζ basis set augmented with diffuse and polarization functions 6-311++G(d,p), and augmented and nonaugmented Dunning's correlation consistent double and triple ζ basis sets[49] (cc-pVDZ, aug-cc-pVDZ, and cc-pVTZ) were used. The tight convergence criteria was used in all cases for the geometry optimizations and the force constants where calculated when necessary.

The stabilization energies were calculated by subtracting the energies of the monomers from those of the complexes and including ZPE (zero point energy) corrections. Most of the energies were also corrected for the BSSE using the counterpoise (CP) scheme of Boys and Bernardi.[50]

To investigate the influence of the BSSE on the geometries of the complexes, all dimers were optimized at the MP2/6-31G(d,p) level of theory using the CP corrections during the optimization process. In addition, the geometries were optimized without BSSE at the same level of theory to compare the influence of the BSSE on the binding energies as well as on the geometries. The small 6-31G(d,p) basis set was selected for this purpose since the BSSE is expected to be more pronounced with small basis sets, and in addition the computations are less demanding.

Results and Discussion

Geometries and Binding Energies. After refining the MMH results, nine furan−FA dimers **A**−**I** were localized at the MP2/6-311++G(d,p) level of theory. For simplicity, in this chapter the geometries and binding energies of the complexes are discussed at this level of theory, whereas the influence of the basis sets on the complexes is discussed later.

The FA molecule exhibits two protons that, in principle, can act as hydrogen bridge donor: the more acidic OH proton and the less acidic aldehyde type CH proton. Consequently, we classify the furan−FA dimers into two types: Type i, where the acidic OH hydrogen atom of FA acts as hydrogen bond donor (dimers **A**, **B**, **C**, and **D1**, Figure 1), and type ii, where the less acidic CH hydrogen atom of FA acts as hydrogen bond donor (dimers **E**, **F1**, **G**, **H**, and **I**, Figure 2).

The complexes **A**−**I** were found being minima using double as well as triple-ζ basis sets. In addition, the five complexes **D**, **D2**, **F**, **K**, and **J** (Figure 3) were only localized at the double-ζ level of theory without augmentation of the basis set. These

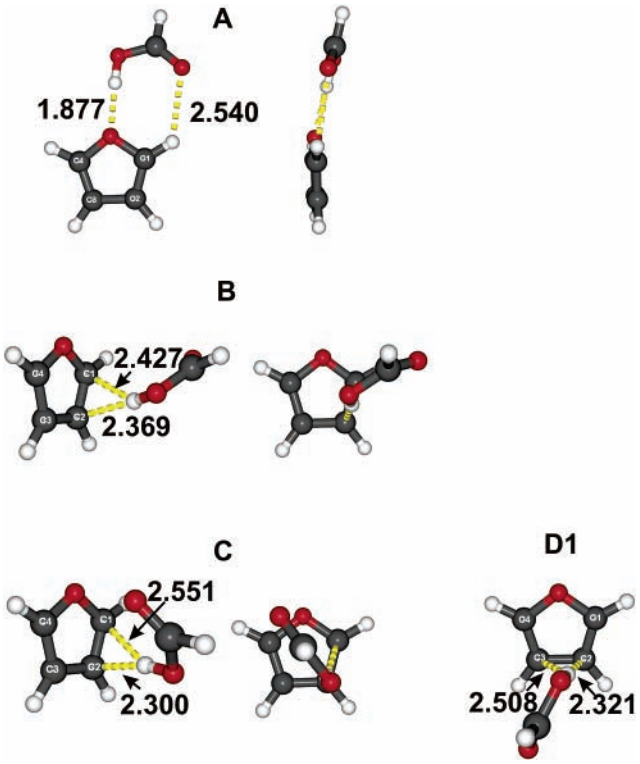

Figure 1. The calculated structures with hydrogen bond lengths (Å) of the type i furan−FA complexes **A**, **B**, **C**, and **D1** at the MP2/6-311++G(d,p) level of theory.

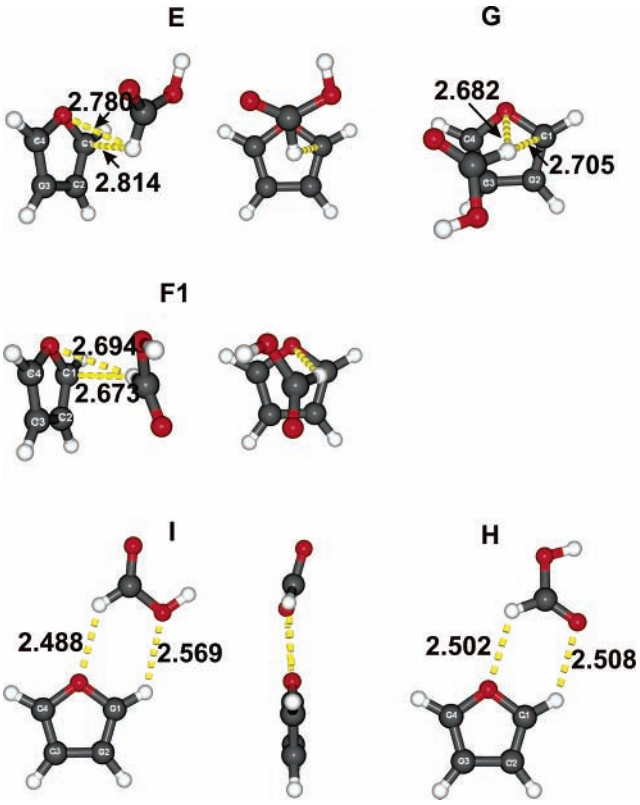

Figure 2. The calculated structures with hydrogen bond lengths (Å) of the type ii furan−FA complexes **E**, **F1**, **G**, **H**, and **I** at the MP2/6-311++G(d,p) level of theory.

complexes do not represent minima at higher levels of theory using larger basis sets.

The interactions between the FA and furan molecules in the complexes can be broken down into six basic interactions 1−6:

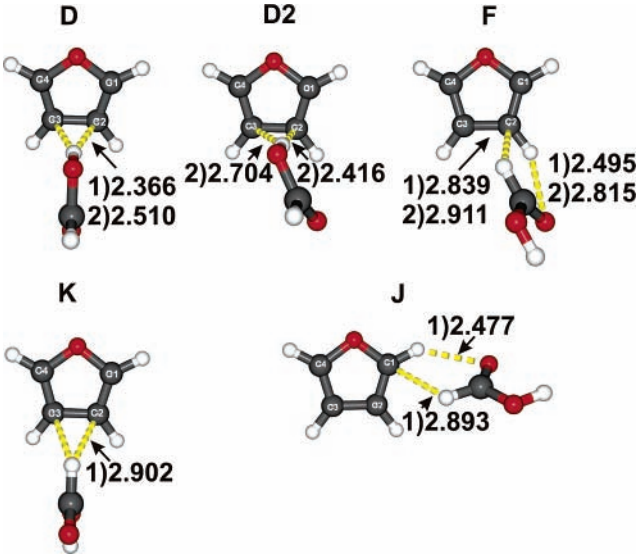

Figure 3. The calculated structures with hydrogen bond lengths (Å) of furan−FA dimers **D**, **D2**, **F**, **J**, and **K** at the MP2/6-31G(d,p) level of theory. (1) Geometry optimized without BSSE corrections. (2) Geometry optimized with BSSE corrections.

(1) O−H_{FA}···nteraction between the hydroxyl hydrogen atom of FA and the oxygen atom of furan.

(2) C═O_{FA}···H_F interaction between the carbonyl oxygen atom of FA and the hydrogen atom of furan.

(3) O−H_{FA}···π interaction between the hydroxyl hydrogen atom of FA and the π system of furan.

(4) C−H_{FA}···O_F interaction between the aldehyde hydrogen atom of FA and the oxygen atom of furan.

(5) H−O_{FA}···H_F interaction between the hydroxyl oxygen atom of FA and the hydrogen atom of furan.

(6) C−H_{FA}···π interaction between the aldehyde hydrogen atom of FA and the π system of furan.

Dimers showing the basic interactions, 1 or 3, involving the acidic OH group of FA are classified as type i complexes, while those showing interactions, 4 or 6, involving the less acidic CH group of FA are classified as type ii complexes. In the complexes, generally more than one of the basic interactions 1−6 are present leading to additional stabilization. The type i complexes **A**−**D** show binding energies between 5.1 and 8.4 kcal/mol, whereas type ii complexes **E**−**K** with binding energies between 2.9 and 4.3 kcal/mol are less stable.

Type i Complexes. The most stable furan−FA dimer is complex **A** with a binding energy of −3.91 kcal/mol at the MP2/6-311++G(d,p) + BSSE + ZPE level of theory (Table 1). The binding energies of all dimers are discussed at this level of theory including BSSE and ZPE corrections unless specified differently. For comparison, selected intermolecular parameters of the dimers **A**−**D2** are shown in Table 2.

The dimer **A** is stabilized by interaction 1 that involves the OH of the FA molecule and the oxygen atom of furan and by interaction 2 between the carbonyl oxygen atom of FA and an α-hydrogen atom of furan. The binding distances and hydrogen bond angles (in parentheses) for interactions 1 and 2 are 1.877 Å (177.87°) and 2.540 Å (124.56°), respectively (Table 2). If dimer **A** is forced to C_s symmetry, it shows one imaginary out-of-plane vibration that after free optimization leads to a slightly distorted equilibrium geometry (Figure 1). The intramolecular bond lengths are not sensitive to this decrease of symmetry in dimer **A**, and the variation of the intermolecular hydrogen bond distances and angles are less than 0.01 Å and 1°, respectively (Table 2). As expected, the binding energy is also hardly affected. Since with other basis sets the C_s symmetrical dimer is a true minimum, the distortion is probably an artifact of the 6-311++G(d,p) basis set.

Dimers **B**, **C**, and **D1** are O−H···π complexes (interaction 3) with very similar binding energies. In dimer **D1** with a binding energy of −2.37 kcal/mol, the OH group of FA interacts with the C2−C3 region of furan. The distances of the OH hydrogen atom to C2 and C3 are 2.321 Å and 2.508 Å, respectively (Figure 1). In the complexes **B** (−2.24 kcal/mol) and **C** (−2.12 kcal/mol), the OH hydrogen atom of FA interacts with the C1−C2 bond of furan. In dimer **B**, the O−H···C2 and O−H···C1 distances are 2.369 Å and 2.427 Å, respectively. In dimer **C**, the O−H···C2 and O−H···C1 distances are 2.300 Å and 2.551 Å, respectively. The main difference between dimers **B** and **C** is the rotation of the FA molecule around its O−H axis (Figure 1). Compared to dimer **B**, the OH hydrogen atom in dimer **C** is closer to atom C2.

Huang et al. calculated the electrostatic potential map of furan at the MP2/6-311++G(d,p) level of theory.[4] Their results indicate that the region with the strongest negative potential is in the vicinity of the O atom. Along the C2−C3 bond, the negative potential is also noticeable. This analysis based on electrostatic potentials agrees well with our results of the type i furan−FA dimers. For the most stable dimer **A**, the OH hydrogen atom of FA interacts with the furan oxygen atom at

TABLE 1: Calculated Binding Energies of the Furan−FA Dimers A−I at the MP2 Level of Theory with the 6-31g(d,p) and 6-311++G(d,p) Basis Sets Including ZPE and BSSE Corrections (in kcal/mol)

	6-31g(d,p) opt with BSSE				6-31g(d,p)				6-311++G(d, p)			
	ΔE	BSSE	ZPE	$\Delta E_{BSSE+ZPE}$	ΔE	BSSE	ZPE	$\Delta E_{BSSE+ZPE}$	ΔE	BSSE	ZPE	$\Delta E_{BSSE+ZPE}$
A	−8.37	2.83	1.01	−4.53	−8.54	3.15	1.11	−4.27	−7.12	2.03	1.18	−3.91
B	−5.16	1.65	0.61	−2.90	−6.05	3.11	0.88	−2.06	−5.51	2.24	1.03	−2.24
C	−5.02	1.80	0.55	−2.67	−5.67	3.00	0.65	−2.02	−5.56	2.42	1.02	−2.12
D	−5.11	1.61	0.48	−3.02	−5.76	2.80	0.64	−2.32			**D1**[a]	
D1			**D2**[a]				**D**[a]		−5.44	2.12	0.95	−2.37
D2	−5.16	1.66	0.54	−2.96			**B**[a]				**D1**[a]	
E	−3.30	1.44	0.55	−1.31	−3.73	2.29	0.64	−0.8	−4.19	2.21	1.02	−0.96
F	−2.89	1.41	0.40	−1.08	−3.17	1.91	0.65	−0.61			**F1**[a]	
F1	−2.89	1.27	0.48	−1.14	−3.21	1.95	0.58	−0.68	−3.76	2.01	0.93	−0.82
G	−2.88	1.27	0.46	−1.15	−3.21	1.96	0.58	−0.67	−3.73	1.99	0.88	−0.86
H	−4.26	1.96	0.56	−1.74	−4.38	2.19	0.67	−1.52	−3.55	1.17	0.44	−1.94
I	−3.40	1.56	0.47	−1.37	−3.50	1.75	0.51	−1.24	−3.05	1.18	0.52	−1.35
J			**H**[a]		−3.37	1.99	0.64	−0.74			**E**[a]	
K			*b*		−2.59	1.59	0.43	−0.57			*b*	

[a] Indicates the dimer that it is found after geometry optimization. [b] Leads to a saddle point structure with two imaginary frequencies.

TABLE 2: Comparison of Selected Intermolecular Parameters in the Furan−FA Dimers A−D2 at Various Levels of Theory[d]

	···MP2					
	6-31G(d,p)$_{BSSE}$	6-31G(d,p)	6-311G++(d,p)	cc-pVDZ	ug-cc-pVDZ	cc-pVTZ
			Dimer **A**			
$OH_{FA}\cdots O_F$	1.973	1.889	1.877 *(1.885)*[a]	1.888	1.859	1.866
$C{=}O_{FA}\cdots H(C1)_F$	2.551	2.416	2.540 *(2.536)*[a]	2.400	2.433	2.447
$<OH_{FA}\cdots O_F$	177.93	176.58	177.87 *(177.53)*[a]	177.43	177.56	178.04
$<C{=}O_{FA}\cdots H(C1)_F$	124.66	124.65	124.56 *(125.26)*[a]	125.25	124.67	124.22
			Dimer **B**			
$OH_{FA}\cdots O_F$	3.074	3.289	2.756	3.225	2.656	2.698
$OH_{FA}\cdots C1_F$	2.566	2.426	2.427	2.409	2.342	2.350
$OH_{FA}\cdots C2_F$	2.432	2.354	2.369	2.328	2.294	2.305
$OH_{FA}\cdots C3_F$	2.907	3.242	2.684	3.167	2.592	2.640
$OH_{FA}\cdots C4_F$	3.234	3.672	2.881	3.579	2.774	2.835
$<OH_{FA}\cdots O_F$	139.14	155.35	124.33	153.96	125.38	127.47
$<OH_{FA}\cdots C2_F$	168.89	159.38	170.44	159.92	171.13	169.91
			Dimer **C**			
$OH_{FA}\cdots O_F$	3.103	2.871	2.961	2.895	2.857	2.871
$OH_{FA}\cdots C1_F$	2.679	2.450	2.551	2.495	2.429	2.426
$OH_{FA}\cdots C2_F$	2.441	2.303	2.300	2.297	2.236	2.253
$OH_{FA}\cdots C3_F$	2.772	2.672	2.610	2.617	2.596	2.638
$OH_{FA}\cdots C4_F$	3.131	2.965	2.970	2.933	2.921	2.957
$C{=}O_{FA}\cdots H(C4)_F$	3.788	3.219	3.365	3.209	3.197	3.313
$<OH_{FA}\cdots O_F$	154.04	144.60	146.22	144.77	145.56	146.72
$<C{=}O_{FA}\cdots H(C4)_F$	125.75	133.29	128.06	131.09	131.47	130.26
$<OH_{FA}\cdots C2_F$	158.89	165.43	165.18	165.32	163.45	163.20
			Dimer **D**			
$C{=}O_{FA}\cdots H(C2)_F$	3.586	2.929	**D1**[b]	2.900	**D1**[b]	3.129
$OH_{FA}\cdots O_F$	3.234	3.359		3.368		3.098
$OH_{FA}\cdots C1_F$	2.967	3.007		3.013		2.816
$OH_{FA}\cdots C2_F$	2.510	2.366		2.359		2.323
$OH_{FA}\cdots C3_F$	2.510	2.366		2.359		2.323
$OH_{FA}\cdots C4_F$	2.967	3.007		3.013		2.816
$<C{=}O_{FA}\cdots H(C2)_F$	102.05	105.46		105.89		104.83
$<OH_{FA}\cdots O_F$	139.35	156.72		156.57		146.91
$<OH_{FA}\cdots C2_F$	163.45	156.84		156.76		159.51
			Dimer **D1**			
$C{=}O_{FA}\cdots H(C3)_F$	**D2**[b]	**D**[b]	3.225	**D**[b]	3.122	3.111
$OH_{FA}\cdots O_F$			2.911		2.845	3.014
$OH_{FA}\cdots C1_F$			2.595		2.487	2.637
$OH_{FA}\cdots C2_F$			2.321		2.230	2.244
$OH_{FA}\cdots C3_F$			2.508		2.476	2.440
$OH_{FA}\cdots C4_F$			2.846		2.818	2.890
$<C{=}O_{FA}\cdots H(C3)_F$			111.40		110.95	108.37
$<OH_{FA}\cdots O_F$			129.68		129.38	141.66
$<OH_{FA}\cdots C2_F$			176.60		178.54	170.14
			Dimer **D2**			
$C{=}O_{FA}\cdots H(C2)_F$	3.255	**B**[b]	**D1**[b]	**D**[b]	**D1**[b]	*c*
$OH_{FA}\cdots O_F$	3.206					
$OH_{FA}\cdots C1_F$	2.769					
$OH_{FA}\cdots C2_F$	2.416					
$OH_{FA}\cdots C3_F$	2.704					
$OH_{FA}\cdots C4_F$	3.150					
$<C{=}O_{FA}\cdots H(C2)_F$	108.22					
$<OH_{FA}\cdots O_F$	138.07					
$<OH_{FA}\cdots C2_F$	176.29					

[a] Geometrical parameters in the C_s symmetry dimer **A**. [b] Indicates the dimer that it is found after geometry optimization. [b] Leads to a saddle point structure with two imaginary frequencies. [c] The geometry was not optimized at this level of theory. [d] Distances are in Å and angles are in degrees.

the site of the strongest negative potential. Dimer **A** is 1.54 kcal/mol more stable than dimer **D1** where the OH hydrogen atom of FA interacts with the C2−C3 bond of furan which indicates a stronger interaction of the acidic hydrogen atom with the furan oxygen atom than with the π system. However, despite that dimer **A** is the electrostatic favored complex, dimers **B**, **C**, and **D1** represent the true prereactive complexes for an electrophilic substitution reaction.

Type ii Complexes. The C−H furan− FA dimers **E**−**I** are very weakly bound complexes (Table 1, Figure 2). Dimers **H** (−1.94 kcal/mol) and **I** (−1.35 kcal/mol) are both C−H···O complexes where the CH hydrogen atom of FA interacts with the lone pairs of the furan oxygen atom (interaction 4) at distances of 2.502 and 2.488 Å, respectively. Dimer **H** in addition is stabilized by interaction 2 between the carbonyl oxygen atom of FA and the α-hydrogen atom of furan (2.508 Å). Complex **I** is stabilized additionally by interaction 5 with an intermolecular distance of 2.569 Å between the OH oxygen atom of FA and a ring hydrogen atom of furan.

Dimers **E**, **F1**, and **G** are energetically very close with binding energies of −0.96, −0.82, and −0.86 kcal/mol, respectively. All of them show a combination of the $C{-}H_{FA}\cdots\pi$ interaction

6 and an atypical C−H···O interaction in the plane of the π orbitals. The C−H···O distances are 2.780 Å, 2.694 Å, and 2.682 Å for the **E**, **F1**, and **G** dimers, respectively. The C−H···C1 distances take values of 2.814 Å, 2.673 Å, and 2.705 Å, in that order. Similarly to dimers **B**, **C**, and **D1**, the dimers **E**, **F1**, and **G** show the formic acid molecule "traveling" around the furan molecule by rotating around its CH axis.

Other Furan−FA Geometries. Two additional type i and three type ii furan−FA dimers **D**, **D2**, **F**, **J**, and **K** were found with smaller basis sets than 6-311++G(d,p) (Figure 3). As mentioned before, at higher levels of theory these complexes do not represent minima. Dimer **D** shows C_s symmetry and at the MP2/6-31G(d,p) + ZPE + BSSE level of theory its binding energy is −2.32 kcal/mol. The O−H···C2 distance is calculated to be 2.366 Å and the O−H···C2 bond angle to be 156.84° (Tables 1 and 2, Figure 3). At the MP2/6-31G(d,p)BSSEopt + ZPE + BSSE level of theory, the binding energy of dimer **D** is −3.02 kcal/mol slightly larger. The O−H···C2 distance is predicted to 2.510 Å, and the hydrogen bond angle is predicted to be 163.45°.

Dimer **D2** could only be localized at the MP2/6-31G(d,p) level of theory if CP BSSE corrections were included during the geometry optimization (Tables 1 and 2). At this level of theory, the binding energy of dimer **D2**, including the ZPE and BSSE corrections, is −2.96 kcal/mol. The O−H···C2 distance is 2.416 Å and the corresponding hydrogen bond angle is 176.29°.

By comparing the structures of dimers **D**, **D1**, and **D2** (Figures 1 and 3), it is clear that **D1** and **D2** are the C_1 symmetrical structures that derive from the C_s symmetrical dimer **D** by tilting and slightly shifting the FA molecule. Of these structures, only the **D1** complex is a minimum at higher level of theory (6-311++G(d,p) and aug-cc-pVDZ basis sets).

The type ii dimers **F**, **K**, and **J** were only localized with the double-ζ basis sets without augmentation. Dimer **F** is a very weak interacting complex with an MP2/6-31G(d,p) + ZPE + BSSE binding energy of −0.61 kcal/mol. At the same level of theory, the $C-H_{FA}\cdots C2_F$ and $C{=}O_{FA}\cdots H_F$ distances are 2.495 and 2.839 Å, respectively. Dimer **F** is mainly stabilized by the weak interaction 2 between the carbonyl oxygen atom of FA and a ring hydrogen atom of furan. Similarly, dimer **J** (−0.74 kcal/mol) is stabilized by interaction 2 with an intermolecular distance of 2.477 Å and by the CH···π interaction where the $CH_{FA}\cdots C1_F$ intermolecular distance is 2.893 Å.

Dimer **K** (−0.57 kcal/mol) exhibits C_s symmetry, and its geometry is much related to the structure of dimer **D** (Figure 3). In dimer **K**, the CH hydrogen atom of FA interacts with the C2−C3 bond of furan. The $C-H_{FA}\cdots C2_F$ distance is 2.902 Å. The larger $A-H_{FA}\cdots C2_F$ (A = O, C) bond length of dimer **K** compared to dimer **D** and the difference between their binding energies (dimer **D** is 1.75 kcal/mol more stable than dimer **K**) are clearly due to the difference in the acidities of the OH hydrogen atom and the aldehyde CH hydrogen atom of the FA molecule.

It is remarkable that both structures **D** and **K** were localized after a procedure on the basis of a completely random exploration of the furan−FA dimers potential energy surface (PES) without any previous chemical assumptions. The most stable furan−FA complex **A** and all the other type i and type ii complexes, as well as their enantiomers, were found using the MMH procedure.

Basis Set Influence on the Calculated Geometries of the Furan−FA Dimers. To analyze the influence of the basis set on the geometries of the furan−FA complexes, the structures of the dimers were optimized using the 6-31G(d,p), 6-311++G(d,p), cc-pVDZ, aug-cc-pVDZ, and cc-pVTZ basis sets. Dimers **A**−**C** are minima with all basis sets (Tables 1 and 3), but only with the 6-311++G(d,p) basis set the equilibrium geometry of dimer **A** deviates from the C_s symmetry plane (Figure 1). Dimer **D1** is only a minimum using the triple-ζ and augmented double-ζ basis sets. With the 6-31G(d,p) basis set, the optimization of complex **D1** leads to **D**, whereas with the 6-31G(d,p) basis set including CP corrections during the geometry optimization dimer **D2** is produced (Table 1).

TABLE 3: Calculated Binding Energies of the Furan−FA Dimers A−I at the MP2 Level of Theory with the cc-pVDZ, aug-cc-pVDZ, and cc-pVTZ Basis Sets Including ZPE Corrections (in kcal/mol)

	cc-pVDZ		aug-cc-pVDZ		cc-pVTZ	
	ΔE	ZPE	ΔE	ZPE	ΔE	BSSE
A	−8.56	1.13	−7.58	1.06	−7.14	1.61
B	−5.93	0.81	−6.85	0.78	−5.73	1.50
C	−5.72	0.65	−6.77	0.76	−5.63	1.57
D	−5.85	0.68	**D1**		−5.65	1.43
D1	**D**		−6.77	0.73	−5.65	1.44
D2	**D**		**D1**		*b*	
E	−3.68	0.60	−5.30	0.82	−3.75	1.15
F	−3.40	0.64	**F1**		b	
F1	−3.14	0.57	−5.06	0.80	−3.44	1.07
G	−3.17	0.57	−5.09	0.82	−3.46	1.06
H	−4.67	0.68	−4.19	0.63	−3.74	1.17
I	−3.73	0.52	−3.45	0.52	−2.90	0.92
J	−3.61	0.64	**E**		*b*	
K	−2.79	0.46	*a*		*b*	

[a] Leads to a saddle point geometry with two imaginary frequencies. [b] The geometry of the complex was not optimized at this level of theory.

The structure **D** was found as a minimum after geometry optimization at the MP2 level with the 6-31G(d,p) (with and without BSSE CP corrections) and cc-pVDZ basis sets. However, when the basis set is augmented by diffuse functions (aug-cc-pVDZ, 6-311++G(d,p)), it becomes a transition state that leads to the equilibrium geometry **D1** (Tables 1 and 3). At the MP2/cc-pVTZ level, dimer **D** is apparently a minimum, but because of the large computational requirements, vibrational spectra were not calculated at this level. Therefore, it is likely that with the cc-pVTZ basis set **D** would become a transition state leading to **D1**, similar to the aug-cc-pVDZ and 6-311++G(d,p) basis sets.

As already mentioned, dimer **D2** could be found only at the MP2/6-31G(d,p) level of theory when including the CP BSSE corrections during the geometry optimization. With the augmented basis sets, dimer **D2** became **D1** after geometry optimization. At the MP2/6-31G(d,p) level without the CP corrections, the geometry optimization of **D2** lead to structure **B**. With the cc-pVDZ basis set, dimer **D2** is converted into dimer **D**, which is a minimum at this level of theory (Tables 1 and 3).

The dimers **E**, **F1**, **G**, **H**, and **I** are minima with all basis sets used (Tables 1 and 3). Complex **I** exhibits C_s symmetry at all levels, except with the 6-311++G(d,p) basis set where it adopts C_1 symmetry (Figure 2). Dimer **F** is found only with the small double-ζ basis sets without augmentation. With the 6-311++G(d,p) and aug-cc-pVDZ basis sets, it transforms to dimer **F1** after geometry optimization (Table 1).

Dimers **J** and **K** were localized only using the cc-pVDZ and 6-31G(d,p) basis sets. When the BSSE correction was included during the geometry optimization (6-31G(d,p) basis set), dimer **J** was transformed to dimer **H** (Table 1). In contrast, with the 6-311++G(d,p) and aug-cc-pVDZ basis sets, the geometry optimization of **J** leads to dimer **E**. Geometry optimization of

TABLE 4: Comparison of Selected Intramolecular Parameters in the Monomer and the Furan−FA Dimers A−D2 at Various Levels of Theory[c]

		MP2				
	experimental[a,b]	6-31G(d,p)	6-311G++(d,p)	cc-pVDZ	aug-cc-pVDZ	cc-pVTZ
			Monomer			
$O-H_{FA}$	0.972	0.972	0.969	0.975	0.975	0.969
$C=O_{FA}$	1.202	1.213	1.205	1.209	1.215	1.203
$C-O_{FA}$	1.343	1.351	1.348	1.350	1.359	1.346
$C1-C2_F$	1.354	1.366	1.370	1.378	1.380	1.364
$C2-C3_F$	1.440	1.427	1.432	1.436	1.438	1.425
$C1-H_F$	1.075	1.075	1.079	1.088	1.087	1.074
$O-C_F$	1.371	1.366	1.360	1.364	1.372	1.359
	6-31G(d,p)BSS E	6-31G(d,p)	6-311G++(d,p)	cc-pVDZ	aug-cc-pVDZ	cc-pVTZ
			Dimer **A**			
$O-H_{FA}$	0.979	0.980	0.977	0.983	0.984	0.978
$C=O_{FA}$	1.216	1.218	1.210	1.215	1.221	1.208
$C-O_{FA}$	1.342	1.339	1.338	1.339	1.347	1.335
$C1-C2_F$	1.364	1.363	1.367	1.375	1.377	1.362
$C2-C3_F$	1.429	1.429	1.434	1.438	1.439	1.427
$C1-H_F$	1.075	1.075	1.079	1.088	1.087	1.075
$O-C1_F$	1.374	1.375	1.370	1.373	1.381	1.368
$O-C4_F$	1.371	1.372	1.367	1.370	1.377	1.364
<C1OC4	106.98	107.15	107.33	107.30	107.38	107.19
			Dimer **B**			
$O-H_{FA}$	0.977	0.978	0.974	0.981	0.982	0.977
$O-C1_F$	1.365	1.365	1.360	1.363	1.370	1.358
$O-C4_F$	1.366	1.366	1.360	1.364	1.372	1.359
			Dimer **C**			
$O-H_{FA}$	0.976	0.977	0.975	0.981	0.983	0.977
$O-C4_F$	1.365	1.364	1.358	1.361	1.369	1.357
			Dimer **D**			
$O-H_{FA}$	0.976	0.977	D1	0.980	D1	0.976
$C2-C3_F$	1.430	1.431		1.439		1.428
			Dimer **D1**			
$O-H_{FA}$	D2	D	0.974	D	0.982	0.977
$C2-C3_F$			1.434		1.440	1.428
			Dimer **D2**			
$O-H_{FA}$	0.976	B	D1	D	D1	
$C2-C3_F$	1.429					

[a] FA ref 57. [b] Furan ref 58. [c] Distances are in Å and angles are in degrees.

complex **K** at the 6-31G(d,p)BSSEopt, aug-cc-pVDZ, and 6-311++G(d,p) levels of theory results in a second-order stationary point (Tables 1 and 3).

Tables 4 and S-1 (see Supporting Information) show some selected intramolecular distances at various levels of theory for the FA−furan dimers. The $C=O_{FA}$ distances decrease up to 0.012 Å when increasing the size of the Pople's basis set from the 6-31G(d,p) to 6-311++G(d,p) whereas the $O-H_{FA}$ and $O-C_F$ distances decrease less, up to 0.005 Å. The $C-H_{FA}$ and $C-H_F$ distances increase with the size of the basis set by around 0.004 Å, and the $C2-C3_F$ distances increase by about 0.005 Å.

With Dunning's basis set at the double-ζ level of theory, the $O-H_{FA}$, $C2-C3_F$, and $C-H_F$ distances are not sensitive to the augmentation. With the augmentation, the $C=O_{FA}$ and $O-C_F$ bond lengths increase by only 0.006 and 0.009 Å, respectively, and the $C-H_{FA}$ distance decreases by about 0.005 Å. These variations are slightly more pronounced if the intramolecular distances calculated with Dunning's double or triple-ζ basis sets are compared. The cc-pVTZ calculated bond lengths are in general shorter than the cc-pVDZ values. Thus, the $C2-C3_F$, $C-H_{FA}$, and $C-H_F$ cc-pVTZ distances are 0.011, 0.015, and 0.013 Å, respectively, shorter than the cc-pVDZ values. The $C=O_{FA}$, $O-H_{FA}$, and $O-C_F$ bond lengths calculated with the triple-ζ basis set are also around 0.006 Å shorter than the cc-pVDZ values.

The intermolecular bond distances and angles of dimer **A** are not very sensitive to the basis set used (Table 2, BSSE effects on the geometries of the complexes are discussed separately). For instance, the $C=O_{FA}\cdots H_F$ distance is 0.12 Å larger in the 6-311++G(d,p) geometry than in the 6-31G(d,p) calculated structure. However, in this case, the 6-311++G(d,p) dimer **A** has C_1 symmetry while the structures of dimer **A** calculated with the other basis sets have C_s symmetry.

Most interesting is the case of dimer **B** where the geometry of the complex shows the largest dependence on the basis set used (Table 2). While the 6-311++G(d,p), aug-cc-pVDZ and cc-pVTZ structures are similar, the geometries calculated with the smaller 6-31G(d,p) and cc-pVDZ basis sets show larger deviations from the higher level structures, although not resulting in new minima. In the structures of complex **B** calculated with the 6-31G(d,p) basis set compared to that with the 6-311++G(d,p) basis set, the $OH_{FA}\cdots C2_F$ hydrogen bond angle is reduced by 11° and the $OH_{FA}\cdots O_F$ hydrogen bond angle increases by 31°. The cc-pVTZ calculated hydrogen bond angles of dimer **D1** also change considerably when compared to the 6-311++G(d,p) and aug-cc-pVDZ calculated values (Table 2). Table 3 shows some selected intermolecular parameters for the dimers **E**−**K** at various levels of theory.

By comparing calculated binding energies of all complexes with the different basis sets, no general conclusion is evident

(Tables 1 and 3). However, the aug-cc-pVDZ calculated binding energies are in general higher than at the other levels of theory, except for dimer **A**. The 6-311++G(d,p) and cc-pVTZ energies are in general in good agreement. Taking into account the compromise between quality of the results and the computational time requirements, we consider that the 6-311++G(d,p) basis set is appropriated for the geometry optimization of these systems. In many cases, the aug-cc-pVDZ basis set provides good geometries too and compares well to the cc-pVTZ and 6-311++G(d,p) results.

Effect of the BSSE on the Calculated Geometries and Binding Energies. BSSE corrections of the binding energies were calculated for all FA−furan dimers at the MP2 level of theory with the cc-pVTZ, 6-311++G(d,p) and 6-31G(d,p) basis sets. With the cc-pVTZ basis set, the BSSE is smaller than with the other basis sets (Tables 1 and 3). With the exception of complexes **F1** and **G**, with Pople's basis sets the BSSE decreases when increasing the size of the basis set from 6-31G(d,p) to 6-311++G(d,p). However, for **F1** and **G**, the differences between the BSSE with the 6-311++G(d,p) and the 6-31G-(d,p) basis sets are very small (0.06−0.03 kcal/mol, Table 1).

To evaluate the influence of the BSSE on the calculated geometries, the structures of all FA−furan dimers were optimized at the MP2/6-31G(d,p) level of theory using the counterpoise (CP)[50] scheme during optimization (6-31G(d,p)-BSSEopt). In contrast to our previous results for other systems[33,37] but in agreement with other studies,[51−53] the BSSE affects the geometry of the complexes in the case of the FA−furan dimers considerably. As already mentioned before, structure **D2** could only be found with the 6-31G(d,p)BSSEopt corrected geometry optimization. Furthermore, the 6-31G(d,p)-BSSEopt optimizations of dimers **D1**, **J**, and **K** lead to entirely different structures compared to those calculated without BSSE corrections (Tables 2 and S-2, Supporting Information). For dimer **K**, the 6-31G(d,p)BSSEopt optimization gave the same structure as with the larger cc-pVTZ, 6-311++G(d,p), and aug-cc-pVDZ basis sets (Tables 1 and 3).

Here, we discuss the 6-31G(d,p)BSSE corrected geometries of the FA−furan dimers compared to the non-BSSE corrected geometries at the same level of theory. As expected, the intramolecular parameters of FA and furan in the complexes were not affected by the inclusion of the BSSE corrections during the geometry optimizations (Table 4 and Table S-1). For the most stable dimer **A**, there is no significant change when including BSSE corrections, only the $OH_{FA}\cdots O_F$ and $C{=}O_{FA}\cdots H_F$ hydrogen bonds are elongated by 0.084 Å and 0.135 Å, respectively (Table 2).

The geometries of other complexes, especially some angles in dimers **B**, **C**, **D**, **F1**, and **G**, are more affected by the inclusion of the BSSE corrections during the geometry optimizations (Tables 2 and S-2). For complexes **D** and **F**, the intermolecular distances increase up to 0.32 Å ($C{=}O_{FA}\cdots H_F$ interaction 2 of complex **F**) when the BSSE is included during the geometry optimization (Figure 3). Our results indicate that the BSSE corrections are more important for the π-bound dimers than for the σ-bound dimers such as **A**, **H**, and **I**. The calculated 6-31G-(d,p)BSSEopt binding energies (without ZPE and BSSE corrections) of **A**, **H**, and **I** agree very well with the 6-31G(d,p) calculated values (Table 1).

Comparison with Other Furan Complexes. All geometries of the FA−furan dimers described in this paper were localized via a random exploration of the multiple minima hypersurface for the furan−FA system without any previous chemical assumptions. It is therefore interesting to discuss structural similarities between these furan−FA dimers and furan homo- and heterodimers found by other methods described in literature.

Pei and Li[2] found four equilibrium isomers of the furan dimer at the B3LYP/6-311G(d,p) level of theory. The most stable structure shows two equivalent CH···O interactions at 2.547 Å and resembles the geometry of the most stable furan−FA dimer **A**. As expected, in dimer **A** the CH···O interaction is stronger than in the furan homodimer. The dimer **A** is stabilized additionally by the $C{=}O_{FA}\cdots H_F$ interaction between the α-hydrogen atom of furan and the carbonyl oxygen atom of FA.

Huang et al.[4] found two geometries for the furan−HX (X = halide) dimers. One is the atom-on type where the H atom of HX interacts with the nonbonding electron pairs of the furan oxygen atom and the HX deviates slightly from the furan ring plane. The other geometry is the face-on type, with a hydrogen bond between the H atom of HX and the π system of furan. For the furan−HF complexes, only the atom-on geometry is observed and for the furan−HI only the face-on type was found. Furan−HCl and furan−HBr dimers exhibit both types of geometries.

Compared to that, the furan−FA complexes **A**, **H**, and **I** show atom-on geometries while dimers **B**, **C**, and **D1** are face-on complexes. The geometries of the furan−HX dimers described by Huang et al. were optimized at the same level of theory (MP2/6-311++G(d,p)) as the furan−FA dimers. It is remarkable that while with others basis sets the equilibrium geometries of dimers **A** and **I** are of C_s symmetry, at the MP2/6-311++G-(d,p) level of theory the geometries deviate from the C_s symmetry. Similarly, the furan−HX dimers deviate slightly from the C_{2v} plane of the furan ring.[4] With both smaller and larger basis sets, a higher symmetry is found, which indicates that the deviation from C_s symmetry is an artifact of the 6-311++G-(d,p) basis set. For instance, at the same level of theory, the C_s geometry of the formamide molecule shows one out-of-plane imaginary frequency resulting again in a slightly distorted structure.

Chan et al.[20] carried out theoretical studies of the reactions of different acids with furan at the MP2/aug'-cc-pVTZ//MP2/6-31+G(d,p) level of theory. They found that hydrogen bonding is largely determined by electrostatic interactions, which generally corresponds to hydrogen bonding to the site with the most localized negative charge. Consequently, the furan molecule forms two hydrogen-bonded complexes with HF, one through a lone pair at the oxygen atom, which is favored, and another dimer through the π system at C2. They found a similar behavior for other weak acids interacting with furan. Depending on the nature of the donor, the π or the O complex is more stable.[20] Huang et al.[4] obtained the atom-on geometry as the only minimum for the furan−HF dimer and the face-on geometry exclusively for the furan−HI complex. This discrepancy between the results of Huang et al. and Chan et al. is an evidence for the difficulties in calculating the weakly interacting complexes of furan.

Matrix Isolation Studies. Matrix isolation spectroscopy allowed to identify and characterize aggregates between FA and furan by IR spectroscopy. The experiments were performed by matrix isolation of mixtures of FA and furan highly diluted in argon at 10 K. Under these conditions (high dilution in argon and slow deposition), the monomers of FA and furan were the main products found in the matrices. Subsequent warming from 10 K up to 35 K allows the matrix-isolated monomers to diffuse and to form aggregates. The main constitutes of the matrices

TABLE 5: Experimental and Calculated Vibrational Frequencies (cm^{-1}) of the Furan−FA Dimer A[c]

			MP2/aug-cc-pVDZ			MP2/6-311++G(d,p)			assignment
M[a]	dimer **A**[b]		M	dimer **A**		M	dimer **A**		
					Formic Acid				
3550.5	3375.2	(−175.3)	3726.7	3543.9	(−182.8)	3797.7	3637.7	(−160.0)	ν(O−H)
	3365.3	(−185.1)							
	3364.2	(−186.3)							
1767.3	1750.3	(−17.0)	1771.0	1755.8	(−15.2)	1807.6	1793.0	(−14.6)	ν(C═O)
1103.5	1150.4	(46.9)	1115.7	1169.2	(53.5)	1142.7	1193.9	(51.2)	ν(C−O)
	1153.0	(49.5)							
					Furan				
1177.7	1167.7	(−10.0)	1218.9	1207.9	(−11.0)	1249.9	1236.2	(−13.7)	ν_{as}(C−O−C)
1065.0	1051.6	(−13.4)	1094.0	1081.4	(−12.6)	1112.5	1095.8	(−16.7)	ν_s(CC) + ν_s(C−O)
993.6	988.3	(−5.3)	1011.4	1006.2	(−5.2)	1025.5	1021.7	(−3.8)	δ(CC−H)
869.1	874.8	(5.7)	865.6	873.3	(7.7)	879.9	885.9	(6.0)	δ_s(C−O−C)
744.1	769.7	(25.6)	742.6	758.3	(15.7)	732.5	748.9	(16.4)	γ(CC−H)
	767.9	(23.8)							
	764.8	(20.7)							

[a] Ar, 10 K. [b] Ar, 10 K, after annealing at 30−35 K. [c] The frequency shifts in dimer **A** compared to furan and FA (monomers M) are given in parentheses.

TABLE 6: Calculated Vibrational Frequencies (cm^{-1}) of the Furan−FA Complexes B−D1[a]

	MP2/aug-cc-p VDZ						
M	complex **B**		complex **C**		complex **D1**		assignment
				Formic Acid			
3726.7	3580.8	(−145.9)	3565.7	(−161.0)	3577.4	(−149.3)	ν(O−H)
1771.0	1758.2	(−12.8)	1757.8	(−13.2)	1757.4	(−13.6)	ν(C═O)
1115.7	1134.8	(19.1)	1140.7	(25.0)	1141.8	(26.1)	ν(C−O)
				Furan			
1218.9	1218.4	(−0.5)	1222.8	(3.9)	1217.3	(−1.6)	ν_{as}(C−O−C)
1094.0	1094.7	(0.7)	1099.2	(5.2)	1094.5	(0.5)	ν_s(CC) + ν_s(C−O)
1011.45	1011.47	(0.02)	1013.3	(1.9)	1011.6	(0.2)	δ(CC−H)
865.6	865.5	(0.1)	865.9	(0.3)	865.6	(0)	δ_s(C−O−C)
742.6	746.9	(4.3)	757.7	(15.1)	744.5	(1.9)	γ(CC−H)
					770.0	27.4	

[a] The frequency shifts in the dimers compared to furan and FA (monomers M) are given in parentheses.

after annealing are the FA dimer, which has been extensively described in literature,[23,54,55] and a complex between furan and FA.

The annealing experiments of argon matrices under various experimental conditions show one new set of IR bands which is only produced in the presence of both furan and FA but not if the matrix is doped with either furan or FA. These new bands show the same relative intensities under all experimental conditions, indicating that they belong to the same molecular species. Consequently, the new bands are assigned to a mixed furan−FA aggregate. The new aggregate is already formed during deposition of a mixture of FA, furan, and argon in a 1:1:1500 ratio on top of a spectroscopic window at 10 K. Annealing of this matrix at 30 K results in a slight increase, and annealing at 35 K in a more pronounced increase of the intensities of the new IR bands (Figures 4−8). By comparison with the spectra calculated for the various furan−FA dimers, these bands were assigned to dimer **A** (Table 5). To suppress the formation of FA dimers, the experiments were also performed with higher concentrations of furan. Under these conditions (FA:furan:Ar = 1:3:1500), the yield of dimer **A** increased and the amount of FA dimers decreased.

The IR spectra of dimer **A** were assigned by comparison with calculations at the MP2/aug-cc-pVDZ and MP2/6-311++G (d,p) levels of theory (Tables 5 and 6). Characteristic for the formation of complexes of FA with hydrogen bonds to the carbonyl group is a red shift of the C═O stretching vibration found in monomeric FA at 1767.3 cm^{-1}. Thus, in the doubly bridged symmetrical dimer of FA, the C═O stretching vibration

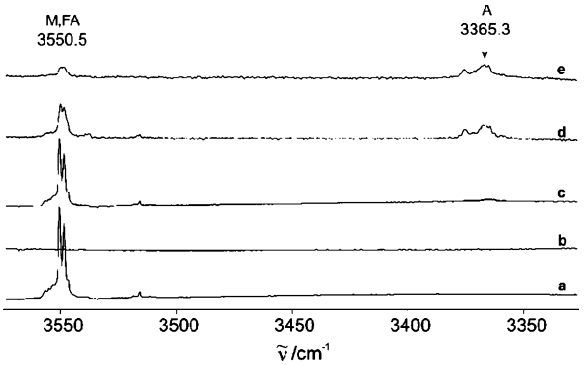

Figure 4. IR spectra in the range 3600−3300 cm^{-1} of FA, furan, and FA/furan mixtures, matrix-isolated in Ar. (a) FA:Ar ratio 1:1500, 10 K. (b) Furan:Ar ratio 1:1500, 10 K. (c) FA:furan:Ar ratio 1:1:1500, 10 K. (d) FA:furan:Ar ratio 1:1:1500 after annealing at 30 K. (e) FA: furan:Ar ratio 1:3:1500 after annealing at 35 K. A: Vibrational modes assigned to the furan−FA dimer.

is red-shifted by −38.6 cm^{-1} [23,54] and in the complex with water by −30.4 cm^{-1}.[35] Two different complexes with dimethyl ether shifts of −32.3 cm^{-1} and −26.1 cm^{-1} were reported.[33] In dimer **A**, a red-shift of −17 cm^{-1} is found. This is in the expected range, although the small value indicates a weaker interaction in **A** than in other FA complexes (Figure 4).

The experimental red-shift is in excellent agreement with calculations both at the MP2/aug-cc-pVDZ and MP2/6-311++G (d,p) levels of theory, which predict shifts of −15.2 and −14.6 cm^{-1}, respectively, for dimer **A**. The red-shift of the C═O

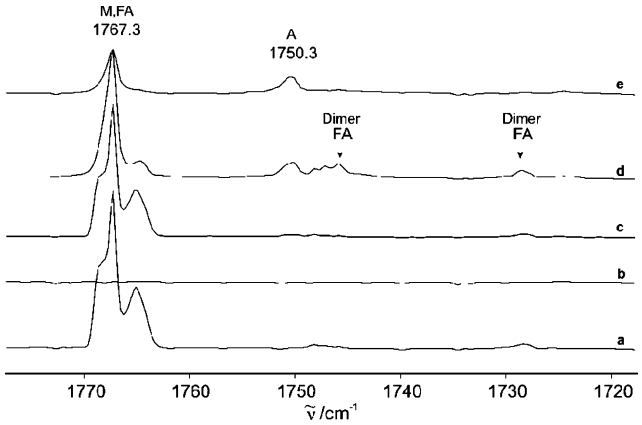

Figure 5. IR spectra in the range 1800−1720 cm^{-1} of FA, furan, and FA/furan mixtures, matrix-isolated in Ar. (a) FA:Ar ratio 1:1500, 10 K. (b) Furan:Ar ratio 1:1500, 10 K. (c) FA:furan:Ar ratio 1:1:1500, 10 K. (d) FA:furan:Ar ratio 1:1:1500 after annealing at 30 K. (e) FA: furan:Ar ratio 1:3:1500 after annealing at 35 K. A: Vibrational modes assigned to the furan−FA dimer.

stretching vibration corresponds to an elongation of the C═O bond by 0.006 Å (6-311++G (d,p) and aug-cc-pVDZ basis sets), because of the formation of the complex (Table 4). For dimer **B**, the red-shift is predicted to −12.8 cm^{-1}, for **C** to −13.2 cm^{-1}, and for **D1** to −13.6 cm^{-1} at the MP2/aug-cc-pVDZ level theory.

The OH stretching vibration of FA at 3550.5 cm^{-1} is split by matrix site effects (Figure 4).[56] Co-deposition of FA, furan, and argon in a 1:1:1500 molar ratio at 10 K and subsequent annealing at 30 K result in the appearance of a new band at 3365.3 cm^{-1} (Figure 4d), which corresponds to a red-shift of −185.1 cm^{-1} from the unperturbed OH mode of FA. Annealing at 35 K for several minutes results in a further increase of the intensity of this band (Figure 4e). Calculations at the MP2/aug-cc-pVDZ and MP2/6-311++G (d,p) levels of theory for dimer **A** predict red-shifts of −182.8 cm^{-1} and −160.0 cm^{-1}, respectively. In particular, the results obtained with the aug-cc-pVDZ basis are in excellent agreement with the experimental data (Table 5).

The formation of dimer **A** results in an elongation of the $O-H_{FA}$ bond length (compared to the FA monomer) by 0.008 and 0.009 Å calculated with the 6-311++G(d,p) and aug-cc-pVDZ basis sets, respectively (Table 4). For dimer **B**, the red-shift is calculated to −145.9 cm^{-1}, for **C** to −161.0 cm^{-1}, and for **D1** to −149.3 cm^{-1} (aug-cc-pVDZ basis, Table 6). These large shifts of the OH stretching vibration allows to discard the FA−furan complexes of type ii without OH...O and OH$\cdots\pi$ interactions, resulting in much smaller perturbations of the OH stretching vibrations (Table 5).

The formation of hydrogen-bonded complexes of FA results in a contraction of the C−OH bond compared to the monomer by 0.010 and 0.012 Å with the 6-311++G(d,p) and aug-cc-pVDZ basis sets, respectively (Table 4), and a blue-shift of the corresponding C−OH stretching vibration (at 1103.5 cm^{-1} in monomeric FA). For dimer **A**, the predicted blue-shift of 53.5 cm^{-1} (aug-cc-pVDZ) nicely matches the experimental value of 46.9 cm^{-1} (Figure 5). For dimer **B**, the shift is calculated to 19.1 cm^{-1}, for dimer **C** to 25.0 cm^{-1}, and for dimer **D1** to 26.1 cm^{-1} (Table 6), in much less agreement with the experimental value and thus confirming the assignment of **A**.

The vibrations of the furan molecule are less affected by the formation of intermolecular complexes. In dimer **A**, the symmetrical and asymmetrical C−O−C stretching vibrations of the furan ring are red-shifted by −13.4 cm^{-1} and by −10 cm^{-1},

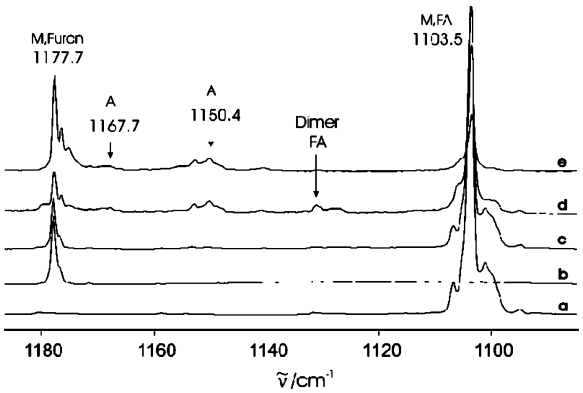

Figure 6. IR spectra in the range 1180−1050 cm^{-1} of FA, furan, and FA/furan mixtures, matrix-isolated in Ar. (a) FA:Ar ratio 1:1500, 10 K. (b) Furan:Ar ratio 1:1500, 10 K. (c) FA:furan:Ar ratio 1:1:1500, 10 K. (d) FA:furan:Ar ratio 1:1:1500 after annealing at 30 K. (e) FA: furan:Ar ratio 1:3:600 after annealing at 35 K. A: Vibrational modes assigned to the furan−FA dimer.

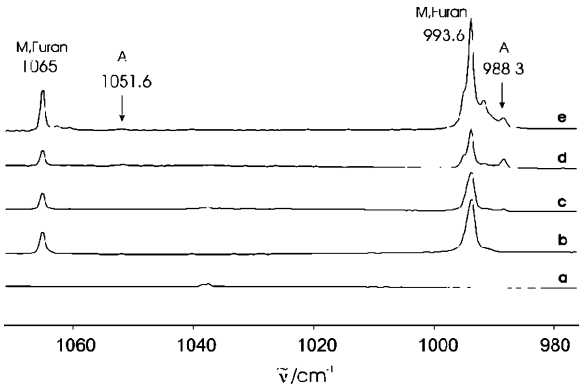

Figure 7. IR spectra in the range 1070−980 cm^{-1} of FA, furan, and FA/furan mixtures, matrix-isolated in Ar. (a) FA:Ar ratio 1:1500, 10 K. (b) Furan:Ar ratio 1:1500, 10 K. (c) FA:furan:Ar ratio 1:1:1500, 10 K. (d) FA:furan:Ar ratio 1:1:1500 after annealing at 30 K. (e) FA: furan:Ar ratio 1:3:600 after annealing at 35 K. A: Vibrational modes assigned to the furan−FA dimer.

respectively (Figures 6 and 7). These experimental shifts are in excellent agreement with the aug-cc-pVDZ calculated values for **A** (Table 5). The CCH deformation mode δ(CCH) of monomeric furan at 993.6 cm^{-1} is shifted to 988.3 cm^{-1} in dimer **A**, which again is in good agreement with the calculation (Figure 7, Table 5). The δ(COC) and γ(CCH) vibration modes are blue-shifted by 5.7 and 25.6 cm^{-1}, respectively (Figure 8). The aug-cc-pVDZ calculations predict shifts of 7.7 and 15.7, respectively, for these vibrations.

Conclusion

Furan is an interesting heterocyclic system that is able to accept hydrogen bonds both in the molecular plane at the basic oxygen atom and perpendicular to the molecular plane at its electron-rich π-system. Formic acid, on the other hand, can act as hydrogen bridge donor either via its acidic OH group or via the less acidic CH group. In addition, it can serve as hydrogen bridge acceptor via its two oxygen atoms. The combination of furan and formic acid thus results in a variety of noncovalently bound dimers which are systematically studied in this paper.

The MMH method, which starts from randomly generated molecular arrangements and which does not require any previous assumptions about the structures of complexes, in combination with high-level ab initio theory, was used to localize and characterize the dimer structures. Nine furan−FA complexes

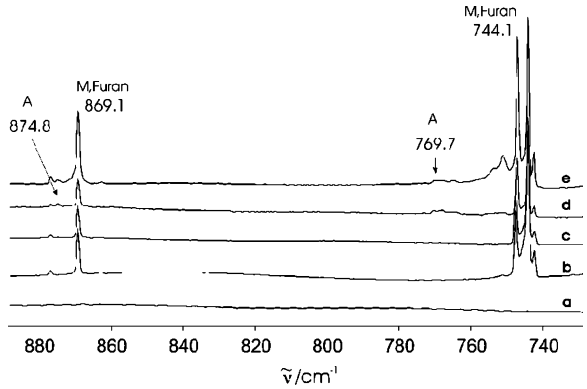

Figure 8. IR spectra in the range 890−740 cm^{-1} of FA, furan, and FA/furan mixtures, matrix-isolated in Ar. (a) FA:Ar ratio 1:1500, 10 K. (b) Furan:Ar ratio 1:1500, 10 K. (c) FA:furan:Ar ratio 1:1:1500, 10 K. (d) FA:furan:Ar ratio 1:1:1500 after annealing at 30 K. (e) FA:furan:Ar ratio 1:3:600 after annealing at 35 K. A: Vibrational modes assigned to the furan−FA dimer.

with binding energies between −3.91 and −0.82 kcal/mol were identified as minima at the MP2/6-311++G(d,p) + ZPE + BSSE level of theory. Another five weaker bound complexes are minima at lower level of theory, only. We classify the furan−FA dimers into two types: type i with the OH hydrogen atom of FA interacting with the furan molecule and type ii where the main interactions are via the CH hydrogen atom of formic acid. Because of the lower acidity of the CH hydrogen atom, type ii complexes are expected to be less stable than type i complexes.

The binding energy of the most stable complex **A** is −3.91 kcal/mol (MP2/6-311++G(d,p) + ZPE+ BSSE, Table 1). Although the OH...O interaction 1 is dominating in dimer **A**, the secondary $C{=}O_{FA}...H_F$ interaction 2 between the carbonyl oxygen atom of FA and the hydrogen atom of furan leads to an additional significant stabilization of this complex. The matrix isolation experiments reveal that dimer **A** is the major, if not only, complex formed if the two monomers are allowed to diffuse slowly in solid argon. The additional IR absorptions that appear in the matrix spectra under these conditions nicely match the theoretical predictions for complex **A**.

Complexes **B**, **C**, and **D1** are π complexes defined by the absence of the strong OH···O hydrogen bond. These dimers are stabilized by the $O{-}H_{FA}{\cdots}\pi$ interaction 2 between the OH hydrogen atom of FA and the π system of furan. With −2.24, −2.12, and −2.37 kcal/mol (MP2/6-311++G(d,p) + ZPE+ BSSE, Table 1), the binding energies are smaller than that of **A**, and consequently these complexes are not identified experimentally. If these complexes are formed in the experiments at all, then their concentration is too low for the experimental identification.

The second group of furan−FA dimers is mainly stabilized by the very weak CH···O or CH···π interactions. The most stable dimers in this group are **H** and **I** with binding energies of −1.94 and −1.35 kcal/mol, respectively, at the MP2/6-311++G(d,p) + ZPE+ BSSE level of theory (Table 1). The higher stability of dimer **H** can be attributed to an additional $C{=}O_{FA}{\cdots}H_F$ interaction between the carbonyl oxygen atom of FA and one of the hydrogen atoms of furan. Dimer **I** exhibits the less stabilizing interaction $HO_{FA}{\cdots}H_F$ between the OH oxygen atom of FA and one of the hydrogen atoms of furan. Dimers **E**, **F1**, and **G** are very weakly bound CH···π complexes with binding energies between −0.96 and −0.82 kcal/mol (MP2/6-311++G(d,p) + ZPE+ BSSE, Table 1).

The MP2 level of theory with the 6-311++G(d,p) and aug-cc-pVDZ basis sets provides reliable geometries for furan−FA complexes. With the small double-ζ basis sets without augmentation, the structures of five additional very weak furan−FA complexes could be localized. Introducing the BSSE corrections during the geometry optimization at the MP2/6-31G-(d,p) level of theory produces variations on the calculated geometries for some of the very weak furan−FA complexes. Here, clearly, BSSE and variations of the basis sets have the largest effects on the dimers. Since the dipole moments and IR spectra very much depend on the structure of the dimers, the experimental identification of these complexes not only requires even milder conditions than matrix isolation but also very carefully selected theoretical methods.

Acknowledgment. This work was financially supported by the Deutsche Forschungsgemeinschaft and the Fonds der Chemischen Industrie. We thank Rachel Crespo for fruitful discussions.

Supporting Information Available: Comparison of selected intra- and intermolecular parameters in furan−FA dimers **E**−**K** at various levels of theory. This material is available free of charge via the Internet at http://pubs.acs.org.

References and Notes

(1) Katritzky, A. R.; Lagowski, J. M. *Heterocycl. Chem.* **1960**.
(2) Pei, K.; Li, H. *J. Mol. Struct.* **2004**, *693*, 141.
(3) Legon, A. C.; Ottaviani, P. *Phys. Chem. Chem. Phys.* **2004**, *6*, 488.
(4) Huang, D. M.; Wang, Y. B.; Visco, L. M.; Tao, F. M. *J. Phys. Chem. A* **2004**, *108*, 11375.
(5) Gromov, E. V.; Trofimov, A. B.; Vitkovskaya, N. M.; Koppel, H.; Schirmer, J.; Meyer, H. D.; Cederbaum, L. S. *J. Chem. Phys.* **2004**, *121*, 4585.
(6) Gromov, E. V.; Trofimov, A. B.; Vitkovskaya, N. M.; Schirmer, J.; Koppel, H. *J. Chem. Phys.* **2003**, *119*, 737.
(7) Cole, G. C.; Legon, A. C.; Ottaviani, P. *J. Chem. Phys.* **2002**, *117*, 2790.
(8) Cooke, S. A.; Corlett, G. K.; Legon, A. C. *Chem. Phys. Lett.* **1998**, *291*, 269.
(9) Cooke, S. A.; Corlett, G. K.; Holloway, J. H.; Legon, A. C. *J. Chem. Soc., Faraday Trans.* **1998**, *94*, 2675.
(10) Montero, L. A.; Gonzalez-Jonte, R.; Diaz, L. A.; Alvarez-Idaboy, J. R. *J. Phys. Chem.* **1994**, *98*, 5607.
(11) Legon, A. C. *Faraday Discuss.* **1994**, *97*, 19.
(12) Alvarez-Idaboy, J. R.; Montero, L. A. *THEOCHEM* **1992**, *85*, 243.
(13) Ault, B. S. *J. Mol. Struct.* **1985**, *127*, 343.
(14) Latajka, Z.; Ratajczak, H.; Orville-Thomas, W. J.; Ratajczak, E. *J. Mol. Struct. (THEOCHEM)* **1981**, *85*, 303.
(15) Koppel, H.; Gromov, E. V.; Trofimov, A. B. *Chem. Phys.* **2004**, *304*, 35.
(16) Alvarez, J. R.; Montero, L.; Martinez, R. *Makromol. Chem.* **1990**, *191*, 281.
(17) Radom, L.; Nobes, R. H.; Underwood, D. J.; Li, W. K. *Pure Appl. Chem.* **1986**, *58*, 75.
(18) DeLaat, A. M.; Ault, B. S. *J. Am. Chem. Soc.* **1987**, *109*, 4232.
(19) Hopkins, B. W.; Tschumper, G. S. *J. Phys. Chem. A* **2004**, *108*, 2941.
(20) Chan, B.; Del Bene, J. E.; Elguero, J.; Radom, L. *J. Phys. Chem. A* **2005**, *109*, 5509.
(21) Legon, A. C.; Millen, D. J. *Faraday Discuss. Chem. Soc.* **1982**, *73*, 71.
(22) Legon, A. C.; Millen, D. J. *Chem. Soc. Rev.* **1987**, *16*, 467.
(23) Halupka, M.; Sander, W. A simple method for the matrix isolation of monomeric and dimeric carboxylic acids. *Spectrochim. Acta, Part A* **1998**, *54A*, 495.
(24) Kim, Y.; Lim, S.; Kim, Y. *J. Phys. Chem. A* **1999**, *103*, 6632.
(25) Priem, D.; Ha, T.-K.; Bauder, A. *J. Chem. Phys.* **2000**, *113*, 169.
(26) Madeja, F.; Havenith, M. *J. Chem. Phys.* **2002**, *117*, 7162.
(27) Galvez, O.; Gomez, P. C.; Pacios, L. F. *J. Chem. Phys.* **2003**, *118*, 4878.
(28) Rozas, I.; Alkorta, I.; Elguero, J. *J. Phys. Chem. B* **2004**, *108*, 3335.
(29) Zhou, Z.; Shi, Y.; Zhou, X. *J. Phys. Chem. A* **2004**, *108*, 813.
(30) Roy, A. K.; Thakkar, A. *J. Chem. Phys.* **2005**, *312*, 119.

(31) Tautermann, C. S.; Loferer, M. J.; Voegele, A. F.; Liedl, K. R. *J. Chem. Phys.* **2004**, *120*, 11650.
(32) Kim, Y. *J. Am. Chem. Soc.* **1996**, *118*, 1522.
(33) Sanchez-Garcia, E.; Studentkowski, M.; Montero, L. A.; Sander, W. *Chem. Phys. Chem.* **2005**, *6*, 618.
(34) Sanchez-Garcia, E.; George, L.; Montero, L. A.; Sander, W. *J. Phys. Chem. A* **2004**, *108*, 11846.
(35) George, L.; Sander, W. *Spectrochim. Acta, Part A* **2004**, *60A*, 3225.
(36) George, L.; Sanchez-Garcia, E.; Sander, W. *J. Phys. Chem. A* **2003**, *107*, 6850.
(37) Sanchez-Garcia, E.; Montero, L. A.; Sander, W. *J. Phys. Chem. A* **2006**, *110*, 12613−12622.
(38) Montero, L. A.; Molina, J.; Fabian, J. *Int. J. Quantum Chem.* **2000**, *79*, 8.
(39) Montero, L. A.; Esteva, A. M.; Molina, J.; Zapardiel, A.; Hernandez, L.; Marquez, H.; Acosta, A. *J. Am. Chem. Soc.* **1998**, *120*, 12023.
(40) Dewar, M. J. S.; Zoebisch, E. G.; Healy, E. F.; Stewart, J. J. P. *J. Am. Chem. Soc.* **1985**, *107*, 3902.
(41) Stewart, J. J. P. MOPAC, v. 6, release for PC computers by L.A.M in the Laboratory of Computational and Theoretical Chemistry, Universidad de La Habana, 1993−1997.
(42) Stewart, J. J. P. *J. Comput. Chem.* **1989**, *10*, 209.
(43) Stewart, J. J. P. *J. Comput.-Aided Mol. Des.* **1990**, *4*, 1.
(44) Frisch, M. J.; Trucks, G. W.; Schlegel, H. B.; Scuseria, G. E.; Robb, M. A.; Cheeseman, J. R.; Zakrzewski, V. G.; Montgomery, J. A., Jr.; Stratmann, R. E.; Burant, J. C.; Dapprich, S.; Millam, J. M.; Daniels, A. D.; Kudin, K. N.; Strain, M. C.; Farkas, O.; Tomasi, J.; Barone, V.; Cossi, M.; Cammi, R.; Mennucci, B.; Pomelli, C.; Adamo, C.; Clifford, S.; Ochterski, J.; Petersson, G. A.; Ayala, P. Y.; Cui, Q.; Morokuma, K.; Malick, D. K.; Rabuck, A. D.; Raghavachari, K.; Foresman, J. B.; Cioslowski, J.; Ortiz, J. V.; Stefanov, B. B.; Liu, G.; Liashenko, A.; Piskorz, P.; Komaromi, I.; Gomperts, R.; Martin, R. L.; Fox, D. J.; Keith, T.; Al-Laham, M. A.; Peng, C. Y.; Nanayakkara, A.; Gonzalez, C.; Challacombe, M.; Gill, P. M. W.; Johnson, B.; Chen, W.; Wong, M. W.; Andres, J. L.; Head-Gordon, M.; Replogle, E. S.; Pople, J. A. *Gaussian 98*, revision A.3; Pittsburgh, PA, 1998.
(45) Frisch, M. J.; Trucks, G. W.; Schlegel, H. B.; Scuseria, G. E.; Robb, M. A.; Cheeseman, J. R.; Montgomery, J. A., Jr.; Vreven, T.; Kudin, K. N.; Burant, J. C.; Millam, J. M.; Iyengar, S. S.; Tomasi, J.; Barone, V.; Mennucci, B.; Cossi, M.; Scalmani, G.; Rega, N; Petersson, G. A.; Nakatsuji, H.; Hada, M.; Ehara, M.; Toyota, K.; Fukuda, R. Hasegara, J.; Ishida, M.; Nakajima, T.; Honda, Y.; Kitao, O.; Nakai, H.; Klene, M.; Li, X.; Knox, J. E., II; Hratchian, P.; Cross, J. B.; Adamo, C.; Jaramillo, J.; Gomperts, R.; Stratmann, R. E.; Yazyev, O.; Austin, A. J.; Cammi, R.; Pomelli, C.; Ochterski, J. W.; Ayala, P. Y.; Morokuma, K.; Voth, G. A.; Salvador, P.; Dannenberg, J. J.; Zakrzewski, V. G.; Dapprich, S.; Daniels, A. D.; Strain, M. C.; Farkas, O.; Malick, D. K.; Rabuck, A. D.; Raghavachari, K.; Foresman, J. B.; Ortiz, J. V.; Cui, Q.; Baboul, A. G.; Clifford, S.; Cioslowski, J.; Stefanov, B. B.; Liu, G.; Liashenko, A.; Piskorz, P.; Komaromi, I.; Martin, R. L.; Fox, D. J.; Keith, T.; Al-Laham, M. A.; Peng, C. Y.; Nanayakkara, A.; Challacombe, M.; Gill, P. M. W.; Johnson, B.; Chen, W.; Wong, M. W.; Gonzalez, C.; Pople, J. A. *Gaussian 03*, revision B.1; Pittsburgh, PA, 2003.
(46) Moller, C.; Plesset, M. S. *Phys. Rev.* **1934**, *46*, 618.
(47) Krishnan, R.; Binkley, J. S.; Seeger, R.; Pople, J. A. *J. Chem. Phys.* **1980**, *72*, 650.
(48) Frisch, M. J.; Pople, J. A.; Binkley, J. S. *J. Chem. Phys.* **1984**, *80*, 3265.
(49) Dunning, T. H., Jr. *J. Chem. Phys.* **1989**, *90*, 1007.
(50) Boys, S. F.; Bernardi, F. *Mol. Phys.* **1970**, *19*, 553.
(51) Crespo-Otero, R.; Montero, L. A.; Stohrer, W.-D.; Garcia de la Vega, J. M. *J. Chem. Phys.* **2005**, *123*, 134107/1.
(52) Salvador, P.; Simon, S.; Duran, M.; Dannenberg, J. J. *J. Chem. Phys.* **2000**, *113*, 5666.
(53) Salvador, P.; Paizs, B.; Duran, M.; Suhai, S. *J. Comput. Chem.* **2001**, *22*, 765.
(54) Gantenberg, M.; Halupka, M.; Sander, W. *Chem.−Eur. J.* **2000**, *6*, 1865.
(55) Reva, I. D.; Plokhotnichenko, A. M.; Radchenko, E. D.; Sheina, G. G.; Blagoi, Y. P. *Spectrochim. Acta, Part A* **1994**, *50A*, 1107.
(56) Lundell, J.; Rasanen, M. *J. Phys. Chem.* **1995**, *99*, 14301.
(57) Harmony, M. D.; Laurie, V. W.; Kuczkowski, R. L.; Schwendeman, R. H.; Ramsay, D. A.; Lovas, F. J.; Lafferty, W. J.; Maki, A. G. *J. Phys. Chem. Ref. Data* **1979**, *8*, 619.
(58) Bak, B.; Hansen, L.; Rastrup-Andersen, J. *Discuss. Faraday Soc.* **1955**, *No. 19*, 30.